Mapping the Universe

MARGARET J. GELLER AND JOHN P. HUCHRA

Maps of the galaxy distribution in the nearby universe reveal large coherent structures. The extent of the largest features is limited only by the size of the survey. Voids with a density typically 20 percent of the mean and with diameters of 5000 km s^{-1} are present in every survey large enough to contain them. Many galaxies lie in thin sheet-like structures. The largest sheet detected so far is the "Great Wall" with a minimum extent of 60 h^{-1} Mpc × 170 h^{-1} Mpc, where h is the Hubble constant in units of 100 km s^{-1} Mpc^{-1}. The frequent occurrence of these structures is one of several serious challenges to our current understanding of the origin and evolution of the large-scale distribution of matter in the universe.

IN THE SECOND CENTURY PTOLEMY WROTE THAT THE GOAL OF map-making is "to survey the whole in its just proportions" and "[to represent] in pictures the whole known world together with the phenomena contained therein" (*1*). With a figurative interpretation of "world," Ptolemy's statement is a remarkably apt description of the aspirations of those of us who are now mapping the universe. This article is a description of some recent explorations.

The foundation for modern maps of the universe is Hubble's 1929 (*2*) discovery that the universe is dynamic. It expands according to the law

$$v_H = H_0 R \tag{1}$$

where v_H is the apparent recession velocity of a galaxy, R is its distance, and H_0 is the Hubble "constant." Cosmological distances are quoted in megaparsecs (1 Mpc = 3.26×10^6 light years). Because the value of H_0 is uncertain by at least a factor of 2, it is often written as $H_0 = 100\ h$ km s^{-1} Mpc^{-1} where h is between 0.5 and 1. Throughout this article we take $h = 1$ unless otherwise specified.

Slipher (*3*) showed that line-of-sight recession velocities could be measured by identifying absorption or emission lines in the spectra of galaxies and measuring the shift of these features toward (generally) longer wavelengths. For the small redshifts, z, we will consider,

$$z = \Delta\lambda/\lambda_r \simeq v/c \tag{2}$$

where $\Delta\lambda = \lambda_0 - \lambda_r$ is the shift of a feature with rest (laboratory) wavelength λ_r observed at wavelength λ_0. One can then make a map of the distribution of galaxies in three-dimensional redshift space. The three coordinates are the two angular positions of a galaxy on the sky and the redshift or apparent recession velocity (cz) along the line-of-sight. In the simplest approximation the redshift of a galaxy provides a measure of its distance. However, "peculiar" velocities complicate the interpretation of the redshift. The measured velocity is

$$cz = H_0 R + v_p = v_H + v_p \tag{3}$$

The peculiar velocities v_p originate from motions of galaxies within gravitationally bound systems and from large-scale coherent flows that may also be gravitationally driven. These peculiar velocities imply that a map in redshift space is a distortion of a map in actual three-dimensional space. In principle, a peculiar velocity for an individual galaxy could be derived from a measurement of the distance to the object along with its redshift. In practice, the measurement of a distance to a galaxy produces a result accurate to only 15% (1σ) whereas redshifts are typically accurate to 0.01%. We discuss the nature of distortions below.

In Hubble's time, measuring a redshift for a nearby galaxy took several hours with a 100-inch telescope. Today with image intensifiers and digital detectors on a 60-inch telescope, similar measurements take only a few minutes. This revolution in detector technology has brought us into an age when we can map the universe (or at least portions of it) in redshift space. In 1956, there were only about 600 galaxies with measured redshifts; in 1976, there were 2,700; in 1980, 5,000; and now, there are more than 30,000. We have now mapped about 10^{-5} of the volume of the visible universe—about the fraction of Earth covered by the state of Rhode Island. Although the coverage is small, the maps contain surprises. The patterns in the distribution of galaxies are larger and more coherent than most of us had expected.

The First Step—A Galaxy Catalogue

The first step in a redshift survey is the construction of a catalogue of positions of galaxies on the sky. These catalogues are magnitude (*4*) or, equivalently, flux limited. During the 1960s Fritz Zwicky and his collaborators (*5*) catalogued the positions of more than 30,000 galaxies brighter than $m_{B(0)} = 15.7$. That catalogue is based on the collection of Palomar Sky Survey plates of the northern sky. This survey was done during the 1950s with the 48-inch Schmidt telescope. Each of the ~1000 plates covers 36 square degrees of the sky. Zwicky and his collaborators examined the plates by eye.

Figure 1, A and B, shows the distribution of galaxies on portions of the sky surveyed by Zwicky *et al.* (*5*). The grid is cartesian in the celestial coordinates α (right ascension) and δ (declination). The galaxies are clearly clustered. Some of the features are well-known gravitationally bound clusters of galaxies. For example, the Coma cluster is the dense concentration at 13^h and 28°. The Virgo cluster, the core of the Local Supercluster, is centered at 12.5^h and 12.5°. The falloff in the density of galaxies west of 9^h and east of 16^h is caused by obscuration in the plane of our galaxy. In the southern

The authors are at the Harvard-Smithsonian Center for Astrophysics, Cambridge, MA 02138.

galactic hemisphere (Fig. 1B) the most prominent feature is the Perseus-Pisces chain which runs across the sky between 30° and 40°. Again the falloff at 21^h and 3^h as well as at the upper range of declination is caused by obscuration in the plane of the Milky Way.

Today more uniform galaxy catalogues reaching to much fainter limits can be constructed by analyzing photodensitometer scans of photographic plates. In one ambitious project, Maddox *et al.* (*6*) have used an automatic plate scanner to extract a catalogue of $\sim 2 \times 10^6$ galaxies covering an area of ~2.5 steradians (sr) in the Southern Hemisphere. The catalogue reaches to a magnitude limit of 20.5 (~150 times fainter than the limit of Zwicky's catalogue) and will, we hope, one day be the basis for a large redshift survey.

Strategies for Redshift Surveys

With a galaxy catalogue in hand, there are still important choices in the design of a redshift survey. Attention to the design of surveys has led to the recent marked advances in our perception of the large-scale distribution of galaxies. Two important parameters of the survey are the geometry and the completeness of sampling. Surveys may be one-dimensional probes to redshifts $z \simeq 0.5$ that cover a very small solid angle on the sky ($\sim 1.5 \times 10^{-4}$ sr) (*7*); these surveys yield samples of the redshift distribution along the line-of-sight. Surveys that cover a large solid angle may be two (*8*) or three dimensional (*9–12*). The depth of a survey (or the flux limit) and the total sky coverage are often most constrained by the availability of time on a telescope of adequate aperture.

The sensitivity to the largest structures is determined by the effective depth and maximum angular scale of a survey. The largest structure that can be detected has a size $\sim \theta D$ where D is the effective depth of the survey and θ is the maximum angle. In other words, a long thin (but not too thin) strip (a two-dimensional survey) is a better configuration for sensitivity to large patterns than a "square" patch that covers the same solid angle.

Recent surveys demonstrate different approaches to the detection of large structures. In 1981 Kirshner, Oemler, Schechter, and Shectman (KOSS) (*13*) discovered the void in Boötes, a region with a diameter of ~ 6000 km s^{-1} where the density of bright galaxies is $\lesssim 20\%$ of the global mean. Low density regions of this scale were unexpected and the discovery created a stir. KOSS (*11*) have now measured redshifts for 239 galaxies in the region of the void. The more extensive survey confirms the existence of a large low density region. Figure 2 is a cone diagram which shows the void (circle). We plot the recession velocity along the radial direction and one of the celestial coordinates along the azimuthal direction. The survey covers a solid angle of ~0.1 sr, but only a small fraction of the galaxies brighter than the limiting flux (~3%) have measured redshifts. Nonetheless, this sparse survey is adequate to provide convincing evidence of a large-scale low density region.

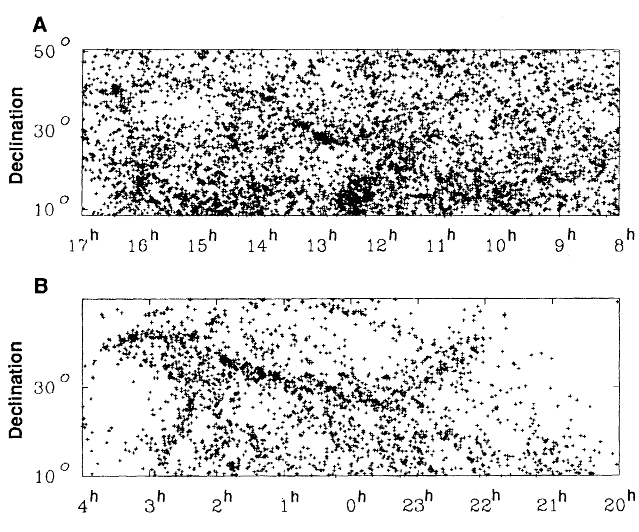

Fig. 1. (**A**) Positions of galaxies in the merged Zwicky-Nilson catalogue with $m_{B(0)} \leq 15.5$ in the northern galactic cap. (**B**) In the southern galactic cap. The coordinates are Cartesian.

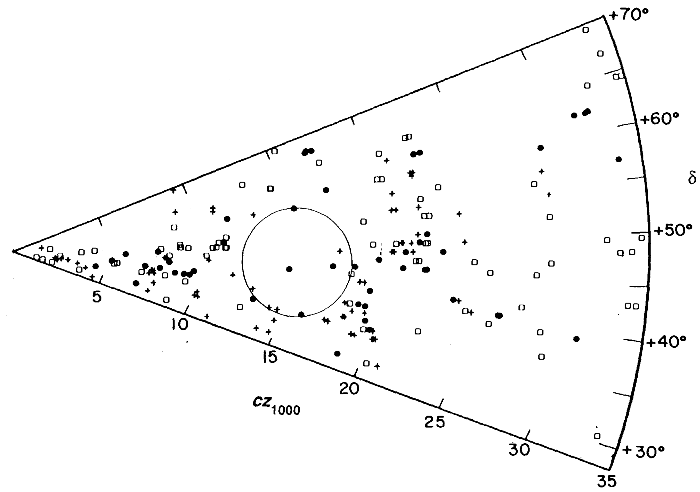

Fig. 2. Cone diagram for the Boötes survey. The circle shows the location of the void; the galaxies within the circle are outside the right ascension range of the void. There are 239 galaxies in the survey (*11*). [Permission to use this figure kindly granted by R. Kirshner]

The KOSS and other surveys suggest some obvious questions. How common are large-scale features in the distribution of galaxies? Given that there are large low density regions, how are galaxies arranged in high density regions? Larger surveys with more dense sampling can now provide partial answers to these questions.

In one approach to these questions, Giovanelli and Haynes (*12*) have been surveying a structure known as the Perseus-Pisces filament (Fig. 1B). A redshift survey over the declination range 30° to 40° shows that many of the galaxies in the region lie in a narrow redshift range centered at about 5000 km s^{-1} (Fig. 3A). Thus the thin structure on the sky is also thin in the redshift direction—hence the designation "filament." The region in the range 22^h to 4^h and from the origin to ~5000 km s^{-1} is a void somewhat smaller than the one in Boötes. This map is much more densely sampled than the one in Fig. 2, but it is not uniformly sampled. Of the 641 redshifts for galaxies in this plot, approximately 250 are from 21-cm observations made at Arecibo. Although our optical survey is only ~50% complete in this region, we measured optical redshifts for about 30% of the galaxies included in the plot.

Recent Results of the CfA Survey

In contrast to the Arecibo survey, the goal of the Center for Astrophysics (CfA) survey is to map the general galaxy distribution rather than to explore a particular apparent feature in the map on the sky. When the survey is complete it will cover the sky at galactic latitudes $b_{II} \gtrsim 30°$ to a limiting magnitude $m_{B(0)} = 15.5$. The galaxy catalogue is essentially the one made by Zwicky. The complete survey will include more than 15,000 redshifts; it will include redshifts for all the galaxies in Fig. 1, A and B. More than 10,000 have already been measured, 75% of these using the 1.5-meter telescope at Mount Hopkins. The typical external error in a redshift is 30 km s^{-1}, which is small compared with the scale of any structure in the survey map.

Surveys like this one are less efficient than the sparse surveys of KOSS for identifying large structures, but they are necessary for quantitative characterization of the distribution of galaxies over a range of scales.

The CfA survey is now complete (or very nearly so) for eight "slices" which include ~5800 galaxies. A "complete" survey is one in which every galaxy brighter than the specified magnitude limit has a measured redshift. A "slice" is a 6°-wide strip (one Palomar Sky Survey plate diameter) at constant declination that spans the full right ascension range of the survey. We observe in slices to discover the large-scale features without having to wait for completion of the entire survey. Observing slices at constant declination is also an efficient use of telescope time.

Figure 3B shows the striking structure in the first slice (completed in 1986) (*8, 14*). The plot includes only the 1,057 galaxies with redshifts ≤15,000 km s^{-1}. Nearly every galaxy in the slice lies in an extended thin structure. The boundaries of the low density voids (regions that contain few bright galaxies) are remarkably sharp and the separation of the galaxies in the boundary structures is generally small compared with the radius of the void. The edges of some of the largest structures may be outside the right ascension range of the survey. At redshifts ≳10,000 km s^{-1} the survey is sparse because the magnitude limited survey includes only the intrinsically brightest galaxies at these redshifts (see the discussion of Fig. 6 below).

The pronounced radial "finger" along the line-of-sight in this slice (the "torso" of the homunculus located at 13^h) is the Coma cluster (see Fig. 1A). If we could map the actual positions of galaxies in space, this feature would be approximately spherically symmetric with a radius of $\sim 1h^{-1}$ Mpc. The elongation in redshift space occurs because galaxies move in the gravitational potential of the cluster with orbital velocities that carry them across the cluster many times (≳10) over the age of the universe. In other words, if the core of the cluster subtends an angle θ on the sky and is at a mean redshift $<v_H>$, the galaxies move with typical line-of-sight velocities σ such that $<v_H>\theta/\sigma << H_0^{-1}$ where H_0^{-1} is approximately the age of the universe. The line-of-sight velocity dispersion for the Coma cluster is ~1000 km s^{-1}. Given the angular size of the system and the velocity dispersion, one can apply the virial theorem to estimate the mass of the system. Such dynamical estimates for cluster masses are larger by about a factor of 10 than the mass of stars responsible for the luminosity of the galaxies in the system. More than 90% of the matter in clusters appears to be dark. This result is called the dark matter problem. Many other groups and clusters of galaxies with a

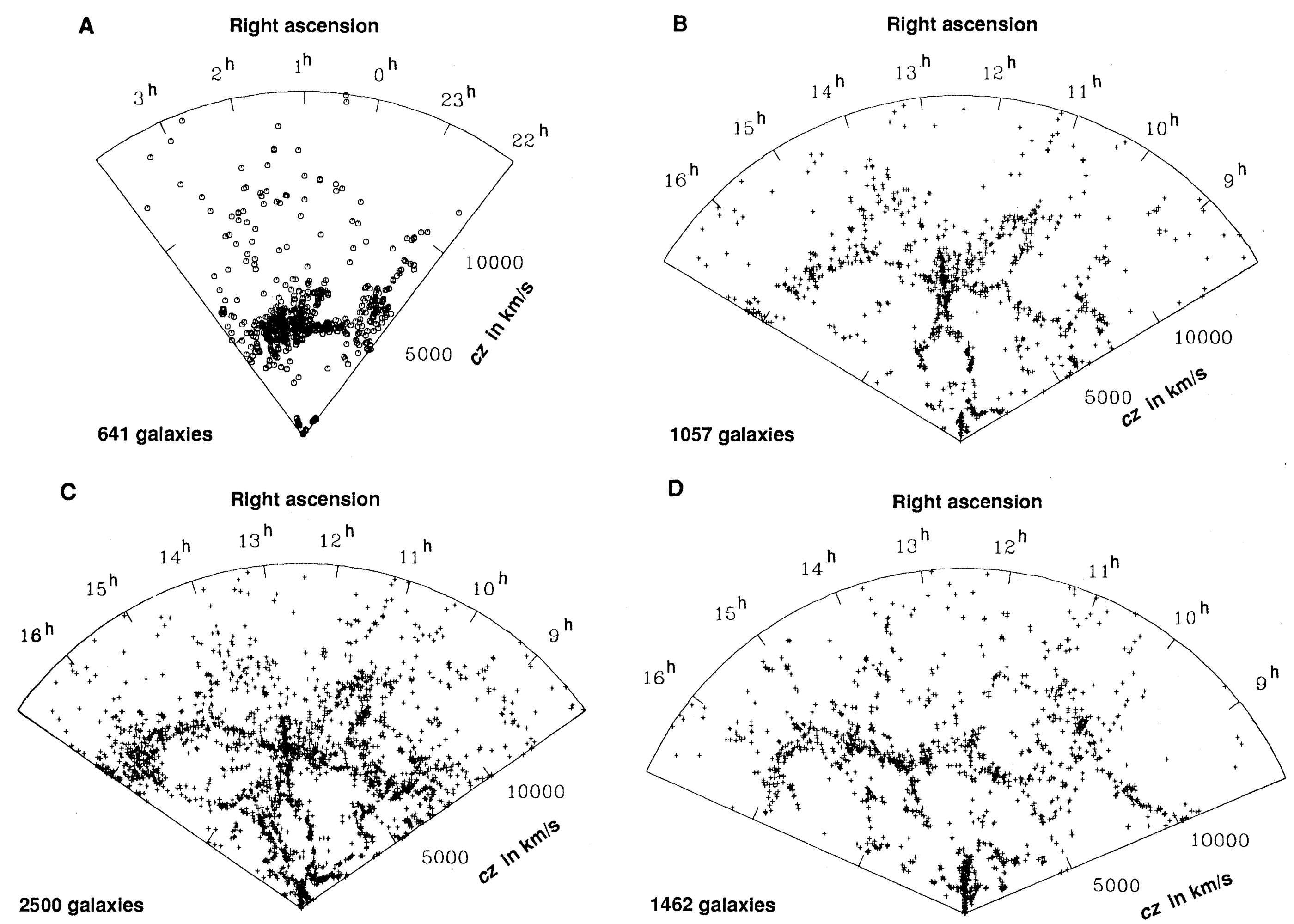

Fig. 3. (**A**) Cone diagram for galaxies in the region of the Perseus-Pisces chain. The data are incomplete. Note the thin, elongated concentration of galaxies at 5000 km s^{-1} and the void that fills the region $cz \lesssim 5000$ km s^{-1}. (**B**) Cone diagram for a complete sample of galaxies with $m_{B(0)} \leq 15.5$ in the declination range $26.5° \leq \delta < 32.5°$. (**C**) Cone diagram for a complete sample covering the declination range $26.5° \leq \delta < 44.5°$. Note the "Great Wall" that runs across the survey. (**D**) Cone diagram for a nearly complete survey of the declination range $8.5° \leq \delta < 14.5°$. Note the correspondence of the wall at ~10,000 km s^{-1} with the structures in (B) and (C). In these diagrams the right ascension is scaled by the cosine of the average declination.

median velocity dispersion of ~200 km s^{-1} are embedded in the thin structures that thread across the survey (*15*). For nearly all of these systems, most of the mass is dark. Estimates of masses for systems of galaxies lead to a value for the cosmological mass density parameter $\Omega = \rho_0/\rho_c = 0.1$ to 0.3 where ρ_0 is the current mean density and $\rho_c = 3H_0^2/8\pi G$ is the critical density, the borderline between unbound ($\Omega < 1$) and bound ($\Omega > 1$) universes.

Although gravitationally bound systems produce local distortions (on scales of a few megaparsecs) of the map in redshift space, removal of these "fingers" does not change the global features of the map on scales of tens of megaparsecs. The first slice alone demonstrates that the thin large-scale features in this region are cuts through two-dimensional sheets, not one-dimensional filaments. In contrast with the situation in Fig. 3A, which samples the apparent filament in Fig. 1B, there is no filament on the sky in the declination range of the slice in Fig. 3B. Furthermore, there are many thin structures in Fig. 3B that run at arbitrary angles with respect to the line-of-sight. The intersection of a slice with a three-dimensional network of filaments is a priori unlikely to be a network of filaments. A network of sheet-like structures that surround (or nearly surround) the voids accounts for the data. The topology could be "bubble-like" or "sponge-like" (*16*)—the maps are not yet extensive enough for clear discrimination among these descriptions. On the basis of maps like those in Fig. 3, A and B, along with similar samples in the Southern Hemisphere, some workers have argued that the galaxy distribution is heterogeneous: it contains filaments, sheets, voids, and diffuse structures (*10, 12*). Maps of other slices in the Perseus-Pisces region (Fig. 1B) show an extension of both the void and the 5000 km s^{-1} ridge of Fig. 3A across a declination range of nearly 40°; the structure here may actually be sheet-like and similar to that in Fig. 3, B to D (*12*). Until all of the surveys can be carefully compared, it will be difficult to judge whether the apparent inhomogeneity is caused by variations in the sampling of the galaxy distribution or by a genuine range in structure.

Additional slices confirm the picture that in the large region covered by the two-dimensional map in Fig. 1A, thin sheet-like structures are the rule. Figure 3C shows an 18°-wide slice which includes the slice in Fig. 3B along with two slices to the north. The distribution of the 2500 galaxies in this slice is still strikingly inhomogeneous. The voids and sheets visible in Fig. 3B are still visible here. The sheets appear thicker here than in Fig. 3B because they are curved or tilted with respect to the plane of this slice.

Because the largest voids in the slice of Fig. 3, B and C, have diameters of ~5000 km s^{-1} and are centered at a redshift of ~7500 km s^{-1}, the declination range required to delimit the void is ~40°. To explore the extent and nature of these features, we followed the completion of the slices in Fig. 3C with a 6°-wide slice covering the declination range $8.5° \le \delta < 14.5°$. This strip is ~160 galaxies short of completion. The most pronounced structure in this strip—the band of galaxies running across the entire right ascension range at velocities between 7500 km s^{-1} and 10,000 km s^{-1}—is once again an extension of the similar feature in Fig. 3, B and C. Unfortunately we do not yet have much data in the 12° strip between the sample in Fig. 3C and the one in Fig. 3D. However, the strong correspondence between the structures in these regions indicates that this sheet spans the entire declination range from 8.5° to 44.5°. Figure 4 shows a three-dimensional view of the four slices. In each of the four slices the "Great Wall" running across the survey between 7,500 km s^{-1} and 10,000 km s^{-1} contains more than half the galaxies in the region.

The apparent extension of the "Great Wall" in both right ascension and declination is only limited by the extent of the survey; we do not yet know the full extent of the structure. The equivalent spatial extent in these two dimensions is ~$60h^{-1}$ Mpc × $170h^{-1}$ Mpc. The typical thickness of these sheets (approximately along the redshift direction) is $\lesssim 5h^{-1}$ Mpc FWHM. The density contrast between this wall and the mean for the survey (as opposed to contrast with the surrounding regions) is $\Delta\rho/\rho \simeq 5$. If we take $\Omega \simeq 0.2$, the mass of this observed portion of the Great Wall is ~2×10^{16} $M_\odot$, a factor of 10 greater than the mass of the Local Supercluster (*17*).

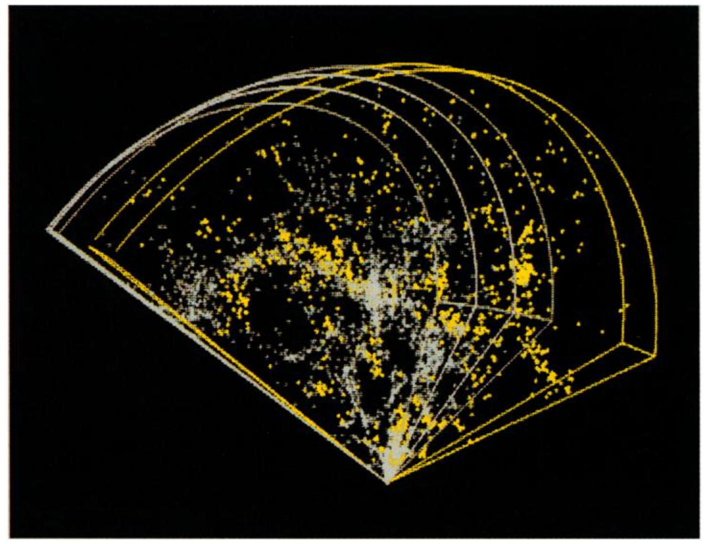

Fig. 4. A three-dimensional view of the maps in Fig. 3, C (white) and D (yellow).

The Great Wall is a demonstration of one of the most sobering results of large redshift surveys: the size of the largest structures we detect is limited only by the extent of the survey. This large-scale inhomogeneity implies that we do not yet have a sample of the universe large enough to determine the typical quantitative characteristics of the three-dimensional distribution of galaxies on scales $\gtrsim 10h^{-1}$ Mpc. We note here that although we have so far treated the Great Wall as a single coherent structure, it could well be made up by the connection of several surfaces that surround (or nearly surround) adjacent voids. In other words, it probably makes more physical sense to regard the individual voids as the fundamental structures. If we started with a uniform distribution, the radii of the voids are the minimum distances we must move points to construct the observed inhomogeneous distribution.

Both large voids and extended sheets appear to be common features of the large-scale distribution of galaxies. Every redshift survey large enough to contain a 5000 km s^{-1} void does—there are now five such surveys. Figure 5, a 360° view (suggested by M. Ramella), shows that thin sheets are also a characteristic feature. Here the data are incomplete; the blank regions are obscured by the galactic plane. However, the plot indicates the geometric relationship between the Perseus-Pisces chain (Fig. 1B) and the Great Wall. Although such features have been qualitatively reproduced in *N*-body models (*18–21*) for the evolution of large-scale structure, it is not yet clear whether they can be matched quantitatively.

One might worry that the structure we observe is somehow an artifact of the way we make galaxy catalogues. Galaxy catalogues are flux limited. The luminosities of galaxies are distributed according to the luminosity function (*22*)

$$\phi(L)dL = \phi^*\left(\frac{L}{L^*}\right)^\alpha \exp\left(\frac{-L}{L^*}\right)d\left(\frac{L}{L^*}\right) \tag{4}$$

where $\phi(L)dL$ is the number of galaxies per unit volume in the luminosity interval $(L, L + dL)$ and L^* and α are constants. For this survey, $\alpha = -1.1$, $L^* = 7.4 \times 10^9 L_\odot$, and $\phi^* \simeq 0.02 \pm 0.005$ h^3

galaxies Mpc^{-3} (*23*). Thus, if galaxies were uniformly distributed in space their distribution in velocity would be given by the curve in Fig. 6. The histogram shows the observed distribution of velocities for the galaxies in the four slices of Fig. 3, C and D, and Fig. 4. Note that at the peak of the expected distribution (~5000 km s^{-1}), the observed distribution is nearly at its minimum value. The broad minimum between ~2,000 km s^{-1} and ~6,000 km s^{-1} is caused by the voids in the galaxy distribution; the peak between ~6,000 km s^{-1} and ~10,000 km s^{-1} is mostly composed of galaxies in the Great Wall.

The catalogue we use was extracted from plates taken in the B band. Samples of galaxies from sky surveys at other wavelengths trace the same structures. There is, for example, a galaxy catalogue made from the survey done by IRAS (Infra-Red Astronomy Satellite). A redshift survey based on this catalogue in the region (*24*) of Fig. 3B shows the same structure we observe in the optical, although more sparsely sampled. Galaxies with emission lines (*25*) and galaxies of low surface brightness (*26*) also trace the same large-scale structure.

Another problem in the interpretation of redshift survey maps is the distortion caused by peculiar velocities other than those caused by motions in bound systems of galaxies. Recently Lynden-Bell *et al.* (*27*) claimed detection of large-scale flows with an amplitude of ~500 km s^{-1} and coherent over a scale of ~$50h^{-1}$ Mpc. They suggested that this large-scale streaming motion is induced by a mass concentration of ~2.5×10^{16} $M_{\odot}$, which they called the "Great Attractor." Redshift surveys in the "Great Attractor" region (*28*) have not yet directly revealed the suggested mass concentration that should be located at a redshift of ~4000 km s^{-1} in the direction ~13.3^h, $-53.4°$. Interestingly the mass of the Great Attractor is comparable with the mass we infer for the *observed* portion of the more distant Great Wall.

We have begun to set limits on large-scale flows in the region of the Great Wall (*29*). To begin to understand the relationship between maps in physical and redshift space, we measured distances [with the I-band infrared Tully-Fisher technique (*30*)] to 40 galaxies on the near and far edges of the void that lies between 4500 km s^{-1} and 9500 km s^{-1} and in the right ascension range 13^h to 17^h of Fig. 3B. We find that the ratio of distances to the near and far edges is 2.08 ± 0.05; the ratio of velocities is 2.19 ± 0.05. The structure of this "bubble" is certainly well-approximated by assuming that the galaxies are on the Hubble flow. In other words, the large-scale structure in redshift space is a close approximation to the structure in real space. This correspondence is also characteristic of the structure produced in the most successful models for large-scale structure. Of course, this measurement applies directly to a single region and does not preclude the existence of other large-scale streaming.

Observations of and/or constraints on the amplitude of large-scale flows can provide important large-scale constraints on the value of Ω. A redshift survey is a map of the distribution of light-emitting matter (galaxies); measurement of peculiar velocities provides constraints on the mass distribution that may differ from the distribution of light. In the linear regime, the peculiar velocity induced by a spherically symmetric mass concentration $\delta\rho/\rho$ is (*31*)

$$\frac{v_P}{v_H} = -\frac{1}{3}\Omega^{0.6}\frac{\delta\rho}{\rho} \qquad (5)$$

A void acts as a negative mass concentration; we thus expect outflow from low density regions and infall toward high density regions. Recently Yahil (*32*) and Dekel and Bertschinger (*32*) have developed methods for recovering the large-scale matter density distribution from surveys that include redshifts and independent distance estimates (these together yield peculiar velocities) for galaxies. In these calculations, Ω is the free parameter. Application of these techniques to existing data [for example, (*27*)] shows that for redshifts $\lesssim$3000 km s^{-1} the derived mass distribution corresponds qualitatively to the observed large-scale galaxy distribution. Extension of these techniques to larger, uniform samples is clearly the route to measuring the relative distribution of dark and light-emitting matter in the universe.

Models for Large-Scale Structure

The observed large-scale features in the galaxy distribution, the dark matter problem, and the detection of large-scale flows are among the important observational constraints on models for the formation and evolution of the large-scale distribution of galaxies.

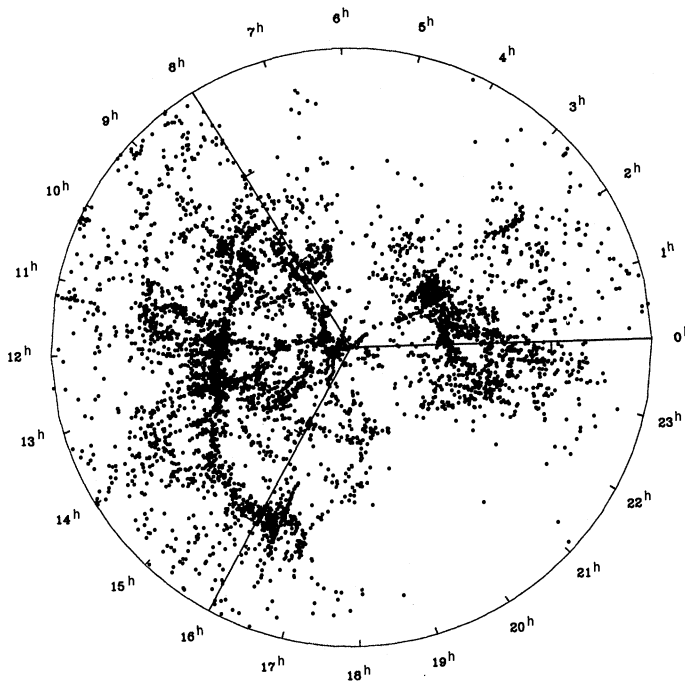

Fig. 5. A 360° view that shows the relationship between the "Great Wall" of Fig. 3, C and D, and the Perseus-Pisces chain of Fig. 3A. This slice covers the declination range $20° \leq \delta < 40°$. It contains all of the available data in the region (6112 galaxies with $cz \leq 15{,}000$ km s^{-1}; the sample is not magnitude limited). The blank regions are obscured by the galactic plane.

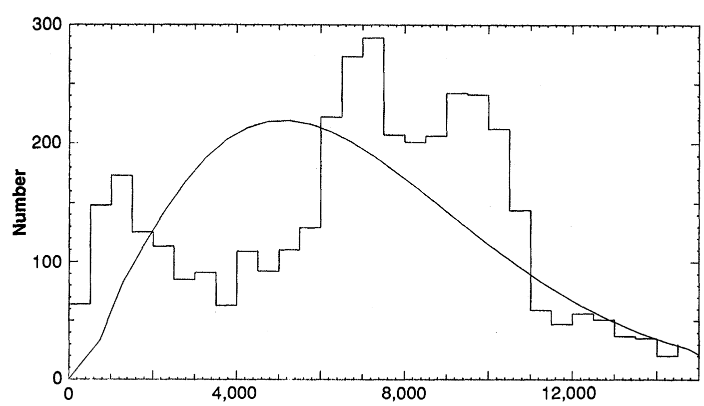

Fig. 6. A comparison of the redshift distribution expected for uniformly distributed galaxies (curve) with the observed distribution (histogram) for the data in Fig. 3, C and D.

Another stringent constraint is the remarkable smoothness of the relic 3 K background. On angular scales from 30″ to 2° the upper limits on temperature fluctuations $\delta T/T \lesssim 2 \times 10^{-4}$ (*33*). The smoothness of the microwave background stands in sharp contrast with the observed large-scale inhomogeneity of the distribution of galaxies.

In the standard picture, the rich large-scale structure we observe today develops by gravitational amplification of small density fluctuations in the early universe. If, as suggested by the application of grand unified theories (GUTs) to the physics of the early universe, the density fluctuations are adiabatic, the fluctuations we now observe in the background radiation are a direct measure of the amplitude of density fluctuations at the epoch when the radiation was last scattered (a redshift $z \simeq 1000$; at approximately this redshift, hydrogen "recombines"). Under the constraint imposed by the small amplitude of the microwave background fluctuations, the most straightforward models, in which all of the matter is baryonic, fail to produce the observed large-scale structure in the galaxy distribution. One obvious loophole in the argument is that the perturbations could be isothermal rather than adiabatic (contrary to the prediction of GUTs).

Dark matter composed of weakly interacting massive particles (WIMPs—none of which have yet been detected) offers the currently preferred solution to the puzzle. Because these particles couple only weakly to the radiation field, perturbations in the "dark matter" can grow at epochs $z \lesssim 1000$ when perturbations in the baryonic component are damped by photon diffusion. After recombination the baryonic matter falls into the potential wells provided by the dark matter. The baryonic material forms the visible portions of galaxies embedded in extended dark haloes.

Results of simulations depend upon the value of Ω, the properties of the dark matter, and the initial spectrum of perturbations in the matter density. The currently most popular model is one dominated by cold dark matter. These particles have low enough velocities to be bound in $\sim 10^8 M_\odot$ perturbations. Davis, Efstathiou, Frenk, White, and others (*21, 34*) have made effective use of *N*-body simulations to carefully examine the prediction of this model. In the models, galaxies form a biased way (*35*): they form where the density contrast exceeds some threshold (like the foam at the peaks of waves in a choppy sea). Without the addition of biasing, the models do not produce sufficiently large voids in the galaxy distribution. The dark matter (perhaps enough to make $\Omega = 1$) is then much more uniformly distributed than the galaxies—the voids are full of dark matter. The matter density contrast is much smaller than the galaxy density contrast we observe. This model succeeds admirably in accounting for many of the properties of individual galaxies, for clustering on scales $\lesssim 10h^{-1}$ Mpc, and for the qualitative appearance of the large-scale galaxy distribution. However, the observations of large-scale streaming toward the Great Attractor and the common occurrence of very large coherent features in the distribution of galaxies are serious challenges.

Hot dark matter provides an obvious alternative (*19*); the candidate particle is the massive neutrino. Here "free streaming" of the particles at the epoch of galaxy formation washes out fluctuations on scales smaller than $\sim 10^{15} M_\odot$; in other words, the velocities of the particles are so large that they are not bound in smaller perturbations. Thus these models can easily yield large structures, but they fail on small scales where they cannot account for the properties of galaxies and individual clusters of galaxies.

A model in which the formation of large-scale structure is driven by explosions (*36*) also accounts for some of the qualitative characteristics of the observed galaxy distribution. Here some set of objects detonates at $7 < z < 100$. The shock fronts from these explosions sweep the ambient gas into thin dense shells that later fragment to form galaxies. This model is less well constrained than the gravitational instability models discussed above. There is no clear candidate for detonation of large enough explosions. Inverse Compton scattering of microwave background photons by the reheated intergalactic medium could produce fluctuations in the microwave background which exceed the upper limits. Large-scale flows have not yet been carefully investigated in this model.

Maps of the galaxy distribution and limits on large-scale flows are important constraints on models for the formation of large-scale structure in the universe. To compare the observed galaxy distribution with models we need (i) statistics that are sensitive to structures on scales $\gtrsim 10h^{-1}$ Mpc, (ii) redshift surveys that are large enough to sample the typical characteristics of the galaxy distribution on these scales (that is, surveys large compared with the features they contain), and (iii) simulations that cover volumes comparable with those of the surveys.

There is a rich literature on the application of correlation function techniques to the measurement of the characteristics of the large-scale galaxy distribution (*6, 37*). However, this low order moment does not provide a satisfactory description of the large coherent features we observe. A statistic that depends upon all moments of the distribution is the void probability function that measures the probability that a randomly selected volume contains no galaxies (*38*). Ostriker and Strassler (*36*) recently used a variant of this statistic to demonstrate the similarity between a simulation of the explosive model and the galaxy distribution in Fig. 3B. A possibly richer route to describing the galaxy distribution is the one taken by Gott *et al.* (*16*) and Ryden *et al.* (*39*), who have suggested statistics that measure the topology of the galaxy distribution. Many of these techniques have not yet been systematically applied to both the available data and the models.

Finally, there are some simple measures that may be discriminatory. The sizes of the largest observed void or coherent sheet are examples. One can measure the probability that such features occur in the models. It is not clear that sufficiently large features occur at all in the models. For example, although 5 out of 5 surveys (*7, 8, 10–12*) contain 5000 km s^{-1} voids, only 3 out of 25 sparsely sampled *N*-body simulations by White *et al.* (*18*) contain a comparable feature. In examining features like the Great Wall, the size of the simulations is a problem. Until very recently, the volumes covered by the simulations were too small to contain such a feature. New simulations by Weinberg and Gunn (*21*) show features that are qualitatively similar to the ones in Figs. 3 and 5.

Conclusions and Prospects for the Future

Maps of the galaxy distribution in the nearby universe reveal large coherent structures. The extent of the largest features is limited only by the size of the survey. Voids with a density typically 20% of the mean and with diameters of 5000 km s^{-1} are present in every survey large enough to contain them. Many galaxies lie in thin sheet-like structures. The largest sheet detected so far is the Great Wall with a minimum extent of $60h^{-1} \times 170h^{-1}$ Mpc. The frequent occurrence of these structures poses a serious challenge for all current models.

The interpretation of the observations of large-scale flows remains somewhat confusing. The mass of the Great Attractor responsible for the flow detected by Lynden-Bell *et al.* (*27*) is comparable with the mass of the Great Wall. Even though the Great Attractor is at less than half the redshift of the Great Wall, it is not easily visible in existing redshift surveys.

In the region of the CfA survey, dynamical estimates yield $\Omega \simeq 0.2$, consistent with earlier determinations (*40*). Interestingly, synthesis of the light elements in the early universe places an upper limit on the cosmological mean baryon density $\Omega_{\text{baryon}} \simeq 0.15$ (*41*). In the most straightforward interpretation of the data, Ω is low and all the matter may be baryonic (note that even with $\Omega \simeq 0.2$ most of the matter is dark).

In part because of the appeal of inflationary cosmology (*42*), models for large-scale structure are most frequently based on $\Omega = 1$ cosmologies. The limits from nucleosynthesis imply that in this case at least 80% of the matter in the universe is nonbaryonic. In these models the matter is more smoothly distributed than the galaxies. The cold dark matter model has been remarkably successful in reproducing many of the salient features of the large-scale galaxy distribution. However, detailed quantitative comparison of the largest scale features may not yield satisfactory results. Larger simulations that can be sampled in the same way as the data are necessary.

The depth and solid angle of redshift surveys are now limited more by the availability of telescope time than by technology or interest. For redshift surveys of the next generation, which might include 100,000 galaxies with $z \lesssim 0.2$, it is desirable to construct a dedicated 4-m class telescope with a 1° field of view. The large field of view enables the use of fiber optics to measure $\gtrsim$100 redshifts at a time.

The equally important distance measurements are a greater challenge. One who discovers a distance estimator good to better than 10% for an individual galaxy would revolutionize the field. Even with current methods, the combination of large samples of distance measurements with complete redshift surveys is a powerful tool for exploring the matter distribution in the universe.

REFERENCES AND NOTES

1. As quoted in J. N. Wilford, *The Mapmakers* (Vintage Books, New York, 1982).
2. E. Hubble, *Proc. Natl. Acad. Sci. U.S.A.* **15**, 168 (1929).
3. V. M. Slipher, *Pop. Astron.* **23**, 21 (1915); later measurements quoted in A. S. Eddington, *Mathematical Theory of General Relativity* (Cambridge Univ. Press, Cambridge, 1923).
4. The magnitude system is the logarithmic scale in which the brightness of a galaxy (or star) is quoted. For two objects with incident fluxes f_1 and f_2 (ergs cm^{-2} s^{-1}) in some band, the difference in the apparent magnitudes of the objects in $m_2 - m_1 = 2.5\log(f_1/f_2)$. On the same scale, the absolute magnitude, M, specifies the intrinsic luminosity of an object in ergs s^{-1}; $m - M = 5\log(d/10\text{ pc})$ where d is the distance to the object in pc and 10 pc is a fiducial distance. The luminosity of a galaxy in the B band referred to the sun is $L(M_B) = 10^{0.4(5.48 - M_B)}\, L_{\odot}$.
5. F. Zwicky, W. Herzog, P. Wild, M. Karpowicz, C. Kowal, *Catalog of Galaxies and of Clusters of Galaxies* (California Institute of Technology, Pasadena, 1961–1968); P. Nilson, *Uppsala General Catalogue of Galaxies, Uppsala Astr. Obs. Ann.* **6** (1973).
6. S. J. Maddox, G. Efstathiou, W. J. Sutherland, J. Lovejoy, in preparation.
7. D. C. Koo, in *Large-Scale Motions in the Universe*, V. C. Rubin and G. V. Coyne, S.J., Eds. (Princeton Univ. Press, Princeton, 1988), pp. 513–560.
8. V. de Lapparent, M. J. Geller, J. P. Huchra, *Astrophys. J.* **202**, L1 (1986).
9. J. P. Huchra, M. Davis, D. W. Latham, J. Tonry, *Astrophys. J. Suppl.* **52**, 89 (1983).
10. L. N. da Costa *et al.*, *Astrophys. J.* **327**, 544 (1988).
11. R. P. Kirshner, A. Oemler, P. Schechter, S. A. Shectman, *ibid.* **314**, 493 (1987).
12. M. P. Haynes and R. Giovanelli, in *Large-Scale Motions in the Universe*, V. C. Rubin and G. V. Coyne, S.J., Eds. (Princeton Univ. Press, Princeton, 1988), pp. 31–70; M. P. Haynes and R. Giovanelli, *Astrophys. J.* **306**, L55 (1986).
13. R. P. Kirshner, A. Oemler, P. Schechter, S. A. Shectman, *Astrophys. J.* **248**, L57 (1981).
14. J. P. Huchra, M. J. Geller, V. de Lapparent, H. G. Corwin, *Astrophys. J. Suppl.*, in press.
15. M. Ramella, M. J. Geller, J. P. Huchra, *Astrophys. J.*, in press.
16. J. R. Gott *et al.*, *ibid.* **340**, 625 (1989).
17. M. Davis and P. J. E. Peebles, *Annu. Rev. Astron. Astrophys.* **21**, 109 (1983).
18. S. D. M. White, C. S. Frenk, M. Davis, G. Efstathiou, *Astrophys. J.* **313**, 505 (1987).
19. J. M. Centrella, J. S. Gallagher, A. S. Melott, H. A. Bushouse, *ibid.* **333**, 24 (1988).
20. D. Weinberg, J. P. Ostriker, A. Dekel, *ibid.* **336**, 9 (1989).
21. D. Weinberg and J. E. Gunn, *Princeton Observatory preprint 316* (Princeton University, Princeton, NJ, 1989).
22. P. Schechter, *Astrophys. J.* **203**, 297 (1976).
23. V. de Lapparent, M. J. Geller, J. P. Huchra, *ibid.* **343**, 1 (1989).
24. B. Smith, S. Kleinmann, J. P. Huchra, F. Low, *ibid.* **318**, 161 (1987).
25. J. J. Salzer, G. S. Aldering, G. D. Bothun, J. M. Mazzarella, C. Lonsdale, *Astron. J.* **96**, 1511 (1988).
26. T. X. Thuan, J. R. Gott, S. E. Schneider, *Astrophys. J.* **315**, L93 (1987).
27. D. Lynden-Bell *et al.*, *ibid.* **326**, 50 (1988).
28. A. Dressler, *ibid.* **329**, 519 (1988).
29. G. D. Bothun, M. J. Geller, J. P. Huchra, R. Schild, in preparation.
30. G. D. Bothun and J. R. Mould, *Astrophys. J.* **313**, 629 (1987).
31. P. J. E. Peebles, *Astrophys. J.* **205**, 318 (1976).
32. A. Yahil, in *Large-Scale Motions in the Universe*, V. C. Rubin and G. V. Coyne, S.J., Eds. (Princeton Univ. Press, Princeton, 1988), pp. 219–255; A. Dekel and E. Bertschinger in *Large Scale Structure and Peculiar Motions in the Universe*, D. W. Latham and L. N. da Costa, Eds. (Astronomical Society of the Pacific, Provo, in press).
33. R. B. Partridge, in *Astronomy, Cosmology, and Fundamental Physics*, M. Caffo, R. Fanti, G. Giacomelli, A. Renzini, Eds. (Kluwer, Dordrecht, 1989), pp. 105–130.
34. M. Davis and G. Efstathiou, in *Large-Scale Motions in the Universe*, V. C. Rubin and G. V. Coyne, S.J., Eds. (Princeton Univ. Press, Princeton, 1989), pp. 439–456.
35. N. Kaiser, *Astrophys. J.* **284**, L9 (1984).
36. S. Ikeuchi, *Publ. Astr. Soc. Jpn.* **33**, 211 (1981); J. P. Ostriker and L. L. Cowie, *Ap. J.* **243**, L127 (1981); J. P. Ostriker and M. J. Strassler, *ibid.* **338**, 579 (1988).
37. P. J. E. Peebles, *Large-Scale Structure in the Universe* (Princeton Univ. Press, Princeton, 1980); M. Davis and P. J. E. Peebles, *Astrophys. J.* **267**, 465 (1983); V. de Lapparent, M. J. Geller, J. P. Huchra, *ibid.* **332**, 44 (1988).
38. S. D. M. White, *Mon. Nat. R. Astron. Soc.* **186**, 145 (1979); J. N. Fry, *Astrophys. J.* **306**, 358 (1986); S. Maurogordato and M. Lachièze-Rey, *ibid.* **320**, 13 (1987); D. H. Weinberg, J. P. Ostriker, A. Dekel, *ibid.* **336**, 9 (1989); M. Vogeley, M. J. Geller, J. P. Huchra, in preparation.
39. B. S. Ryden *et al.*, *Astrophys. J.* **340**, 647 (1989).
40. A. Dressler, in *Astronomy, Cosmology, and Fundamental Physics*, M. Caffo, R. Fanti, G. Giacomelli, A. Renzini, Eds. (Kluwer, Dordrecht, 1989), pp. 23–40.
41. M. S. Turner, in *ibid.*, pp. 279–286.
42. L. F. Abbott and S.-Y. Pi, *Inflationary Cosmology* (World Scientific, Singapore, 1986).

43. We thank E. Falco and R. McMahan for writing the software for the color graphics. We also thank B. Estus and M. Kurtz for advice on graphics. We thank E. Horine, A. Michel, J. Peters, and S. Tokarz for their assistance in data acquisition, reduction, and cataloging. This research was supported in part by NASA grant NAGW-201, by a grant from the Scholarly Studies Program of the Smithsonian Institution, and by the Digital Equipment Corporation.